Article

Cell Reports

CENP-A Is Dispensable for Mitotic Centromere Function after Initial Centromere/Kinetochore Assembly

Graphical Abstract

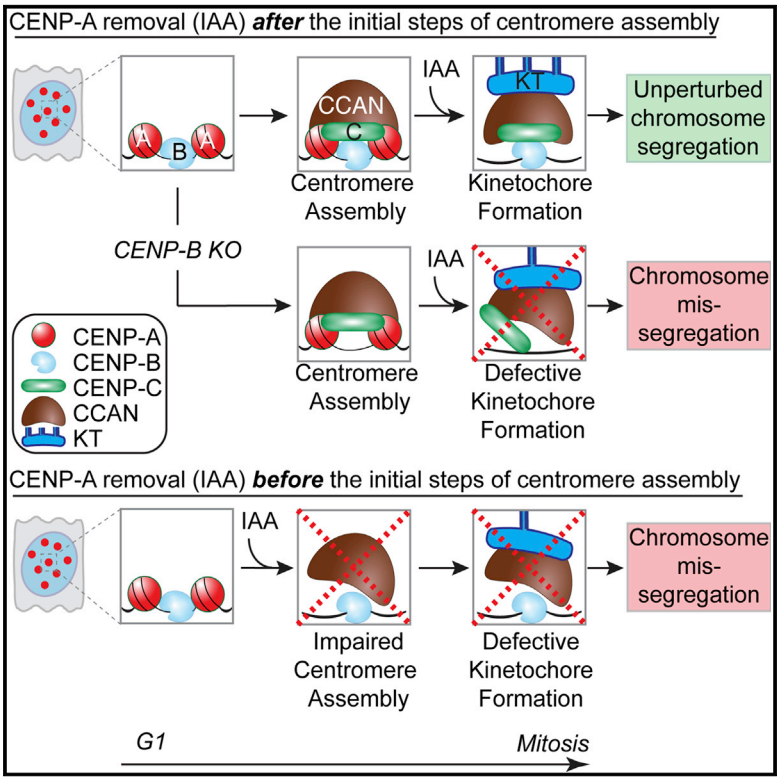

Highlights

- Rapid and complete loss of endogenous human CENP-A using an auxin-inducible degron
- Kinetochore attachment to the centromere is maintained following loss of CENP-A
- After the initial steps of centromere assembly, CENP-A is dispensable for mitosis
- Faithful chromosome segregation by CENP-A-depleted kinetochores requires CENP-B

Authors

Sebastian Hoffmann, Marie Dumont, Viviana Barra, ..., Solène Hervé, Don W. Cleveland, Daniele Fachinetti

Correspondence

dcleveland@ucsd.edu (D.W.C.), daniele.fachinetti@curie.fr (D.F.)

In Brief

Using inducible degradation to remove endogenous CENP-A from human centromeres, Hoffmann et al. show that CENP-A is dispensable for mitotic centromere function after it has mediated the initial steps of centromere and kinetochore assembly. The authors demonstrate that the kinetochore is tethered to the centromere by a dual link: CENP-A chromatin and CENP-B-bound DNA.

Hoffmann et al., 2016, Cell Reports *17*, 2394–2404
November 22, 2016
http://dx.doi.org/10.1016/j.celrep.2016.10.084

CellPress

OPEN ACCESS
CellPress

Cell Reports
Article

CENP-A Is Dispensable for Mitotic Centromere Function after Initial Centromere/Kinetochore Assembly

Sebastian Hoffmann,[1,4] Marie Dumont,[1,4] Viviana Barra,[1] Peter Ly,[2,3] Yael Nechemia-Arbely,[2,3] Moira A. McMahon,[2,3] Solène Hervé,[1] Don W. Cleveland,[2,3,*] and Daniele Fachinetti[1,5,*]
[1]Institut Curie, PSL Research University, CNRS, UMR 144, 26 rue d'Ulm, F-75005, Paris, France
[2]Ludwig Institute for Cancer Research
[3]Department of Cellular and Molecular Medicine
University of California at San Diego, La Jolla, CA 92093, USA
[4]Co-first author
[5]Lead Contact
*Correspondence: dcleveland@ucsd.edu (D.W.C.), daniele.fachinetti@curie.fr (D.F.)
http://dx.doi.org/10.1016/j.celrep.2016.10.084

SUMMARY

Human centromeres are defined by chromatin containing the histone H3 variant CENP-A assembled onto repetitive alphoid DNA sequences. By inducing rapid, complete degradation of endogenous CENP-A, we now demonstrate that once the first steps of centromere assembly have been completed in G1/S, continued CENP-A binding is not required for maintaining kinetochore attachment to centromeres or for centromere function in the next mitosis. Degradation of CENP-A prior to kinetochore assembly is found to block deposition of CENP-C and CENP-N, but not CENP-T, thereby producing defective kinetochores and failure of chromosome segregation. Without the continuing presence of CENP-A, CENP-B binding to alphoid DNA sequences becomes essential to preserve anchoring of CENP-C and the kinetochore to each centromere. Thus, there is a reciprocal interdependency of CENP-A chromatin and the underlying repetitive centromere DNA sequences bound by CENP-B in the maintenance of human chromosome segregation.

INTRODUCTION

A correct balance of chromosome distribution following cell division is a prerequisite for normal development. Indeed, whole-chromosome aneuploidy is responsible for many human genetic diseases and cancer. Centromeres are fundamental for chromosome inheritance, serving as the unique chromosomal locus for the assembly of the kinetochore, a multi-subunit structure that attaches to spindle microtubules, and for centromeric cohesion prior to sister chromatid separation (Fukagawa and Earnshaw, 2014).

From fission yeast to humans, centromeres are epigenetically identified by chromatin assembled with the histone H3 variant CENP-A, a key component of all centromeres (McKinley and Cheeseman, 2016). CENP-A is required and essential to preserve centromere position (Fachinetti et al., 2013) by directing its self-replication at mitotic exit of every cell cycle (Jansen et al., 2007; Shelby et al., 1997) through the histone chaperone HJURP (Dunleavy et al., 2009; Foltz et al., 2009). Key determinants of this function are the CENP-A targeting domain (CATD) (Black et al., 2004) together with the amino- and carboxy-terminal tails that mediate kinetochore assembly (Fachinetti et al., 2013; Logsdon et al., 2015). Indeed, CENP-A has been reported to directly interact with several subunits of the constitutive centromere-associated network (CCAN) onto which the kinetochore is formed (Hori et al., 2008; Foltz et al., 2006; Okada et al., 2006; Cheeseman and Desai, 2008; Izuta et al., 2006; Carroll et al., 2009; Carroll et al., 2010; Fachinetti et al., 2013; Kato et al., 2013; Guse et al., 2011). However, whether CENP-A is necessary for maintaining the kinetochore and, consequently, required for proper chromosome segregation is unclear. Efforts to either reduce CENP-A levels via small interfering RNA (siRNA)-mediated silencing over a 2-day period or eliminate new CENP-A synthesis by gene disruption (7 days to achieve complete depletion) suggested that both the CCAN and the entire kinetochore complex would rapidly disassemble upon loss of anchoring to CENP-A (Régnier et al., 2005; Liu et al., 2006; Fachinetti et al., 2013). Consequently, the pathways for kinetochore assembly were studied in cells by artificially tethering centromeric components to Lac operator (LacO) arrays to bypass the CENP-A requirement (Gascoigne et al., 2011; Logsdon et al., 2015), which was thought to act as an essential connection between chromatin and kinetochore.

Because CENP-A is a long-lived protein (Smoak et al., 2016; Fachinetti et al., 2013) and is essential for maintenance of centromere identity, without ability to induce its rapid depletion at known points in the cell cycle, effects on centromere maintenance and kinetochore function following CENP-A loss cannot be separated from CENP-A's known role in specifying centromere position. Consequently, the importance of centromeric chromatin containing CENP-A in kinetochore maintenance and chromosome segregation has remained untested. In this article, we now develop an approach to allow rapid (<1 hr), inducible

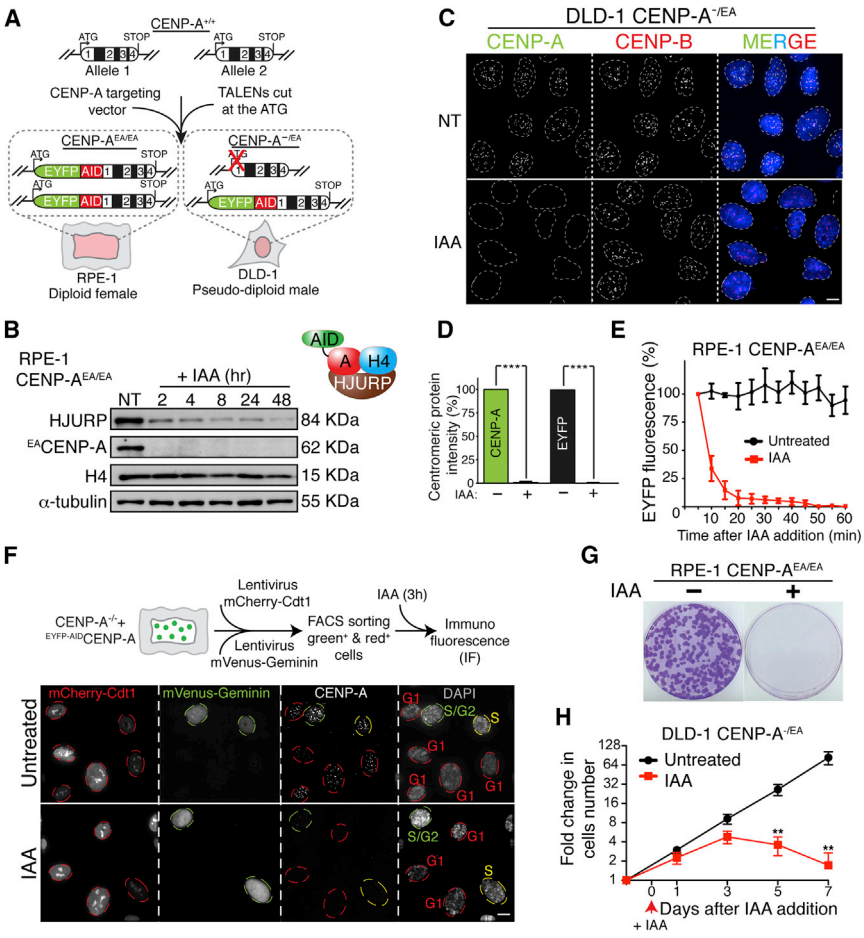

Figure 1. Complete and Rapid Removal of the Centromere Epigenetic Mark CENP-A in Human Cells

(A) Schematic of the TALEN-mediated genome editing strategy to endogenously tag CENP-A with AID (A) and EYFP (E) in the indicated cell lines. Position of exons, introns, and start/stop codons are indicated.

(B) Immunoblot of RPE-1 cells following treatment with Auxin (IAA) at the indicated time points (hours). α-Tubulin was used as a loading control. A schematic of the soluble CENP-A-associated factors is also shown.

(C) Representative immunofluorescence images on DLD-1 cells showing CENP-A depletion after 24 hr treatment with IAA. CENP-B was used to mark centromere position.

(D) Quantification of the experiment in (C) by using an antibody against CENP-A or by monitoring EYFP intensity. Unpaired t test: ***$p < 0.0001$.

(E) Degradation kinetics of CENP-A in RPE-1 cells with or without (+/−) IAA treatment measured by EYFP intensity during live-cell imaging. IAA was added at the microscope stage. n = 10 cells.

(F) Representative images show immunofluorescence on RPE-1 cells expressing the cell-cycle indicator FUCCI. Red (G1), yellow (S), or green (S/G2) circles indicate the cell-cycle position ± IAA treatment. A schematic of the experimental design is also shown.

(G) Images of representative crystal-violet-stained colonies from the colony formation assay ± IAA treatment in RPE-1 cells.

(H) Cell counting experiment on DLD-1 CENP-$A^{-/EA}$ cells ± IAA treatment. IAA was added at day 0 and kept for a maximum of 7 days.

Error bars represent the SEM of five independent experiments. Unpaired t test: **$p = 0.0026$. See also Figure S1. Scale bars, 5 μm.

degradation of the endogenous CENP-A at every stage of the cell cycle. Although overall CENP-A is essential for centromere function, induced degradation of CENP-A demonstrates that after initial centromere assembly, continued CENP-A binding to centromeric chromatin is dispensable for preserving centromere-bound kinetochores. In CENP-A-depleted centromeres, maintenance of kinetochore and centromere attachment and high-fidelity chromosome segregation in the next mitosis is dependent on CENP-B.

RESULTS

Rapid and Complete Depletion of the Endogenous CENP-A in Human Cells

To produce cells whose centromeres would be supported by an inducible degradable CENP-A, we used genome editing to add amino-terminal EYFP and auxin-inducible degron (AID) tags to endogenous CENP-A to facilitate its rapid and complete depletion in human cells (Nishimura et al., 2009; Holland et al., 2012). We did this by (1) modifying both endogenous *CENP-A* alleles with amino-terminal EA (enhanced yellow fluorescent protein [EYFP]-AID) tags in a diploid, non-transformed human RPE-1 cell line, or (2) tagging one allele and inactivating the other in a pseudo-diploid colorectal human cancer DLD-1 cell line (Figure 1A; Figures S1A and S1B). Additionally, in both *CENP-*$A^{EA/EA}$ and *CENP-*$A^{-/EA}$ cell lines, a gene encoding the plant E3 ubiquitin ligase osTIR1 was stably integrated to enable rapid degradation of AID-CENP-A upon addition of the synthetic auxin indole-3-acetic acid (IAA). Fusion of the AID and EYFP tags to one or both *CENP-A* alleles did not interfere with CENP-A or centromere function, as long-term maintenance of cell viability was found in CENP-A-deficient RPE-1 (*CENP-*$A^{-/-}$) cells when rescued with a $^{EYFP\text{-}AID}$CENP-A transgene (Figures S1C–S1E).

Auxin addition led to complete depletion of all endogenous CENP-A protein, measured using three complementary approaches: immunoblotting (using anti-CENP-A and anti-GFP antibodies; Figure 1B; Figure S1F), immunofluorescence (using anti-GFP and an anti-CENP-A antibody; Figures 1C and 1D; Figure S1G), and immunoprecipitation (following chromatin precipitation with an anti-GFP antibody; Figures S1H–S1J). Loss of CENP-A appeared complete at individual centromeres (we have previously demonstrated that our immunofluorescence approach could identify as little as one molecule [Fachinetti et al., 2013], starting from the initial 400 molecules per human centromere [Bodor et al., 2014]). Importantly, complete degradation of CENP-A was also observed (by immunofluorescence

using a CENP-A antibody recognizing amino acids [aa] 3–19) on C-terminal-tagged CENP-A (CENP-$A^{3HA\text{-}AID}$), demonstrating that the entire protein was removed from centromeres (Figure S1G).

CENP-A depletion occurred rapidly (with first-order kinetics) and to completion within 50 min, with a half-life of 9 min (Figure 1E; Figure S1K; Movie S1) in all examined cell lines and at every stage of the cell cycle (with cell-cycle position visualized using the fluorescence cell-cycle indicator [FUCCI] reporter system [Sakaue-Sawano et al., 2008] or by arresting cells in mitosis with a microtubule depolymerizing drug; Figure 1F; Figure S1L). CENP-A degradation also triggered rapid, partial degradation of its pre-nucleosomal assembly factor HJURP (Foltz et al., 2009; Dunleavy et al., 2009) (Figure 1B), in agreement with the reciprocal stabilization of the CENP-A^{CID}/$HJURP^{CAL1}$ complex observed in flies (Bade et al., 2014). As expected, CENP-A depletion led to cell lethality in both RPE-1 and DLD-1 cells as observed by a colony-forming assay (a 2-week growth assay; Figure 1G; Figure S1M). However, surprisingly, cell death was not immediate, but initiated after the second cell cycle, presumably from rampant chromosome mis-segregation (Figure 1H).

CENP-A Is Dispensable for Kinetochore Maintenance and Chromosome Segregation during Mitosis, but Essential for Overall Centromere Function

To address whether CENP-A-depleted centromeres retained their function in mediating chromosome attachment to mitotic spindle microtubules, we followed chromosome segregation by live-cell imaging (after stable insertion of mCherry-H2B) in cells that underwent a first or second round of mitosis without CENP-A (2 or 24 hr of IAA treatment, respectively; Figure 2A). Remarkably, no significant increase in chromosome segregation defects was observed in RPE-1 *CENP-*$A^{EA/EA}$ cells with auxin-induced degradation of CENP-A in the 2 hr preceding the first mitosis (Figure 2B, 2 h IAA). On the other hand, after 24 hr (about one full cell cycle) without CENP-A, cells that entered mitosis had severe accumulation of mis-aligned chromosomes, extended mitotic duration, and subsequent formation of micronuclei at mitotic exit (Figures 2B and 2C). Importantly, the frequency of mis-segregated chromosomes was dependent on when in the cycle CENP-A was depleted. CENP-A depletion during G1 produced the highest error frequency in the first mitosis after CENP-A degradation, with a much lower error rate when CENP-A was depleted from S-phase cells and an even lower rate when depleted in G2 (Figure 2D; Figures S2A and S2B).

We then investigated the consequences of CENP-A depletion on binding of centromere and kinetochore components and on the kinetochore capture of spindle microtubules. We measured the binding stability of several components of the CCAN (including CENP-B, CENP-C, CENP-T, and CENP-I) in interphase or of the mature kinetochore in mitosis (including Dsn1, a subunit of the Mis12 complex, and Hec1, a subunit of the Ndc80 complex) following CENP-A depletion for either 2 or 4 hr or for an entire cell cycle (24 hr) (Figures 2E–2G). CENP-A depletion for 4 hr resulted in only a minor reduction in interphase on all measured centromere-bound components except CENP-C (Figure 2F), which underwent an immediate, substantial (~70%) reduction. CENP-T and CENP-I levels at centromeres significantly decreased in cells only following an entire cell cycle without CENP-A (Figures 2F and 2G). Centromere-bound CENP-B also slightly diminished following CENP-A depletion (Figure 2F), consistent with direct stabilization of CENP-B via the CENP-A amino-terminal tail (Fachinetti et al., 2013; Fachinetti et al., 2015).

Similarly, degradation of CENP-A within 2 hr of mitotic entry left binding of components of the mature mitotic kinetochore, Dsn1 and Hec1, almost unchanged. In cells entering mitosis 24 hr (i.e., one cell cycle) after CENP-A depletion, both Dsn1 and Hec1 were reduced (by ~50%; Figure 2G). Microtubules were still stably bound to kinetochores in the absence of CENP-A (4 or 24 hr after addition of IAA), as observed by immunofluorescence following cold treatment to disassemble all but kinetochore microtubules (Figure S2C).

Altogether, these findings revealed a dual response to CENP-A depletion immediately prior to cell division: it is dispensable for kinetochore maintenance and chromosome segregation in the first mitosis, but essential to preserve centromere function in a subsequent cell cycle. The reduced binding stability of centromere and kinetochore components following CENP-A depletion for 24 hr is likely to be the primary deficit that leads to severe chromosome mis-segregation in CENP-A-depleted centromeres.

CENP-A Is Critical for Initial Assembly of Centromeric Components CENP-C and CENP-N, but Not CENP-T

We next tested whether the severe chromosome segregation defects in mitosis following an entire cell cycle without CENP-A (24 hr treatment) could be the result of failure of centromere assembly. First, we tested the dependency of loading of new molecules of CENP-C—known to directly interact with CENP-A (Carroll et al., 2010; Kato et al., 2013; Falk et al., 2015) and to be recruited at ectopic sites by CENP-A/HJURP (Logsdon et al., 2015; Tachiwana et al., 2015)—on the continued presence of CENP-A at native centromeres. For this, we tagged a single *CENP-C* allele with RFP-AID to follow its localization at CENP-A-containing or CENP-A-depleted centromeres (Figures 3A–3C). After IAA treatment to induce CENP-C or both CENP-C/CENP-A degradation (Figure 3C, red bars) and IAA removal to permit re-accumulation of CENP-C and/or CENP-A, respectively (see immunoblot in Figure S2D), new CENP-$C^{mRFP\text{-}AID}$ deposition at centromeres was measured in cells released from G1 cell-cycle arrest. Despite continued presence of CENP-B at centromeric loci following CENP-A degradation, CENP-$C^{mRFP\text{-}AID}$ failed to re-localize to centromeres in CENP-A-depleted cells following IAA removal (Figures 3B and 3C, solid versus striped light blue bars; Figure S2E). Taken together, these findings reveal a requirement for CENP-A, but not for CENP-B, for new CENP-C loading at native centromeres.

Moreover, we found that deposition of new CENP-C occurred within a window of a few hours after mitotic exit (determined using live-cell imaging on *CENP-*$C^{+/AE}$ cells released from mitotic block [nocodazole] or S-phase block [thymidine], or in untreated conditions; Figures S2F–S2H). Therefore, we conclude that CENP-C loading takes place only a few hours after CENP-A deposition (Figure S2I) and is dependent on CENP-A.

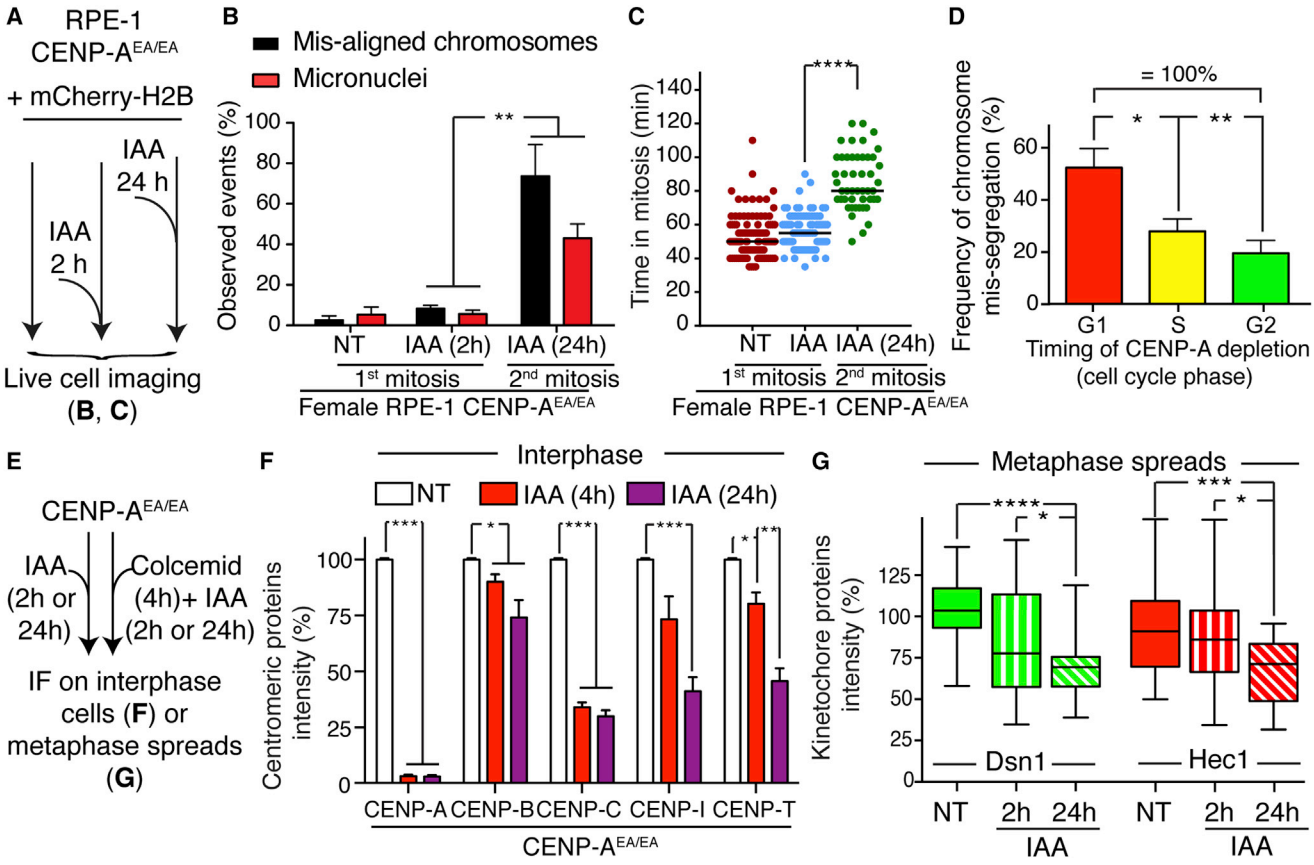

Figure 2. CENP-A Is Dispensable for Centromere and Kinetochore Maintenance and Chromosome Segregation Once Centromere Is Assembled

(A) Schematic of the experiments shown in (B) and (C).

(B) Bar graph shows the percentage of chromosome mis-segregation events by live-cell imaging in non-treated conditions or following IAA treatment for 2 or 24 hr, respectively. Error bars represent the SEM of three independent experiments. Individual n = ~35 cells. Unpaired t test: **p = 0.0099 and 0.0065.

(C) Each individual point represents a single cell. Time in mitosis was defined as the period from nuclear envelope breakdown (NEBD) to chromosome decondensation. Error bars represent the SEM of three independent experiments. Unpaired t test: ****p < 0.0001.

(D) Bar graph shows the frequency of chromosome mis-segregation (micronuclei and mis-aligned chromosomes, 2 hr IAA treatment condition) versus the cell-cycle phase in which CENP-A was depleted (determined by measuring the time required for the cells to enter into mitosis in asynchronous population, using cell co-expressing $PCNA^{GFP}$ as an indicator of the cell cycle or by synchronizing cells in G1 by adding IAA either at t = 0 hr or at t = 9 hr) in DLD-1 cells. Unpaired t test: *p = 0.0142, **p = 0.0024.

(E) Schematic of the experiments shown in (F) and (G).

(F) Bar graphs showing centromere intensities of CENP-A, CENP-B, CENP-C, CENP-I, and CENP-T for the indicated cell line following IAA treatment. Values represent the mean of six independent experiments combining analysis performed in RPE-1 and DLD-1 cells. Individual N = ~30 cells, N = 25 centromeres per cell. Error bars represent the SEM. Unpaired t test: ***p < 0.0001, **p < 0.07, *p < 0.05.

(G) Box and whisker plots of Dsn1 or Hec1 intensities at the centromere measured on metaphase spreads.

Unpaired t test: *p = 0.017, ***p = 0.0005, ****p < 0.0001. See also Figure S2.

We then measured CENP-N and CENP-T stability and their deposition in CENP-A-depleted cells using the SNAP-tag method (Jansen et al., 2007; Bodor et al., 2012) (Figures 3D–3G). Both CENP-N and CENP-T are essential components for centromere function (Foltz et al., 2006; McKinley et al., 2015), and their depletion causes a strong mitotic arrest within 2 hr of IAA addition (Figure S2J; Wood et al., 2016). Surprisingly, following CENP-A depletion and release into S-phase, pre-deposited $CENP\text{-}N^{3HA\text{-}SNAP}$ (labeled by covalent linkage to tetramethylrhodamine [TMR]) remained stably bound to centromeres (Figures 3E and 3F). In contrast, new CENP-N failed to deposit at CENP-A-depleted centromeres (Figures 3E and 3F) as observed by initial addition of bromothenylpteridine (BTP; a non-fluorescent substrate used to block subsequent visualization of all pre-deposited SNAP-tagged molecules) followed by new protein synthesis labeled by the SNAP substrate TMR. Pre-deposited centromeric CENP-T was reduced following CENP-A depletion, but its deposition was not prevented in the absence of CENP-A (Figure 3G). Taken together, these results show that CENP-A itself is required for new assembly of CENP-C and CENP-N, but not of CENP-T. However, CENP-A is not necessary in the short term for CENP-N maintenance once already assembled at centromeres.

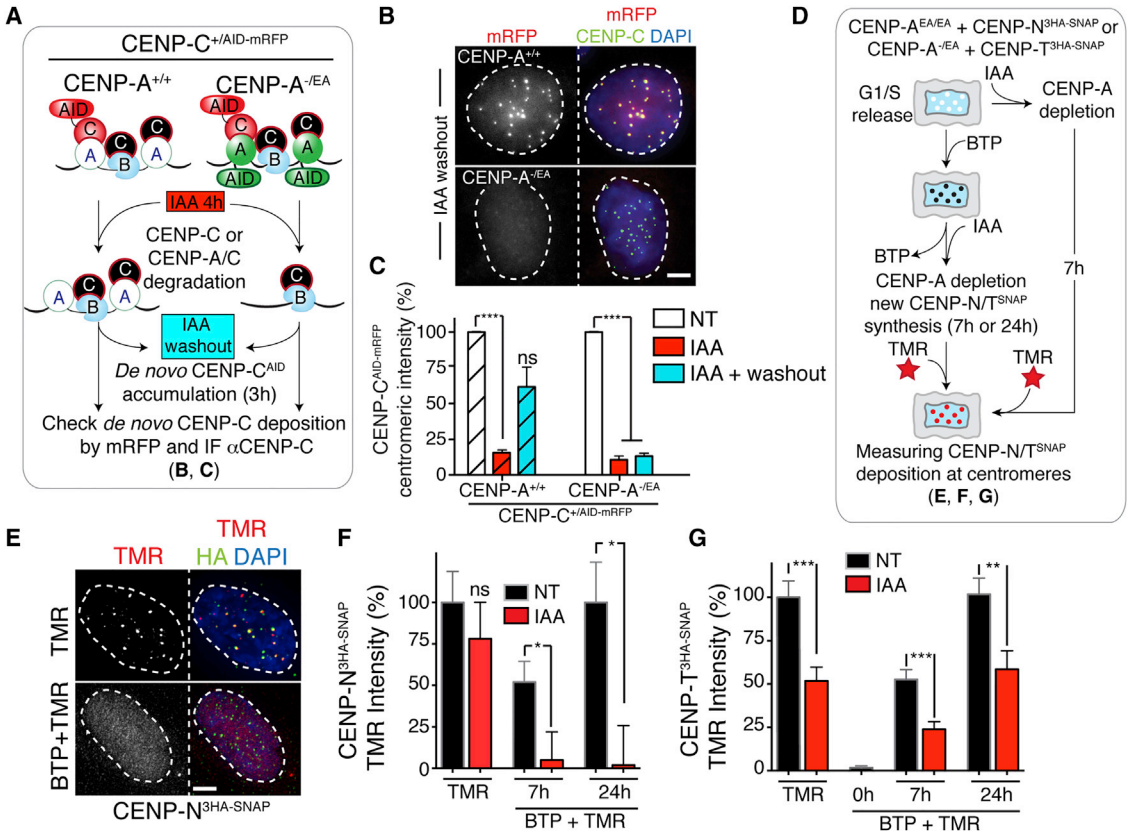

Figure 3. CENP-A Is Required to Regulate Early Steps of Centromere Assembly, Such as for CENP-C and CENP-N, but Not CENP-T

(A) Schematic of the experiments shown in (B) and (C).

(B) Representative immunofluorescence images show de novo CENP-$C^{AID\text{-}mRFP}$ loading at centromeres.

(C) Bar graphs showing centromere intensities of CENP-$C^{AID\text{-}mRFP}$ in the indicated cell lines. Error bars represent the SEM of three independent experiments. Individual N = ~30 cells, n = 25 centromeres for cell. Unpaired t test: ***$p < 0.0001$.

(D) Schematics of the experiments shown in (E)–(G).

(E) Representative immunofluorescence images show de novo CENP-$N^{3HA\text{-}SNAP}$ loading at centromeres. Hemagglutinin (HA) antibody was used to identify unlabeled CENP-N.

(F and G) Bar graphs showing centromere intensities of CENP-$N^{3HA\text{-}SNAP}$ or CENP-$T^{3HA\text{-}SNAP}$, respectively, in the indicated cell lines. Values represent the mean of three independent experiments. Error bars represent the SEM. Individual n = ~30 cells, n = 25 centromeres for cell. Unpaired t test: *$p = 0.01$, **$p = 0.0028$, ***$p = 0.0003$.

See also Figure S2. Scale bars, 5 μm.

CENP-B Binding to Alphoid DNA Is Necessary and Sufficient for Kinetochore Anchoring via CENP-C on CENP-A-Depleted Centromeres

Previously, we demonstrated that the Y chromosome recruits less CENP-C and mis-segregates at a higher rate compared with the X chromosome or any of the autosomes (Fachinetti et al., 2015). We suggested that this inherent instability could be due to the complete absence of CENP-B binding boxes in the Y chromosome's centromeric sequences (Earnshaw et al., 1989; Miga et al., 2014), which represent the sites for the centromeric DNA binding protein CENP-B. Indeed, alone among the human chromosomes, the Y does not have the CENP-B-mediated backup pathway for maintenance of CENP-C at its centromere (Fachinetti et al., 2015).

Consistent with this, the first mitosis following CENP-A depletion in male DLD-1 cells was accompanied by an overall increase in chromosome segregation defects compared with RPE-1 cells (Figure S3A). Detailed analysis revealed that, on average, in most cells in the first mitosis after CENP-A degradation, one chromosome failed (or delayed) in alignment to metaphase, whereas two or more were mis-aligned in the second mitosis after removal of CENP-A (Figure S3B). Fluorescence in situ hybridization (FISH) analysis revealed that depletion of CENP-A resulted in a significant accumulation of micronuclei (MN) carrying the Y chromosome (~36% of MN+Y; one cell out of seven cells carried a Y chromosome in MN; Figure 4A) accompanied by the loss of centromere-bound CENP-C as observed by both immunofluorescence (IF)-FISH (Figure 4B) and chromatin immunoprecipitation (ChIP) analysis on CENP-C (Figure S3C). In agreement with our previous findings (Fachinetti et al., 2015), even in cells with normal CENP-A levels there was already a selective reduction of CENP-C binding to the Y centromere compared with other

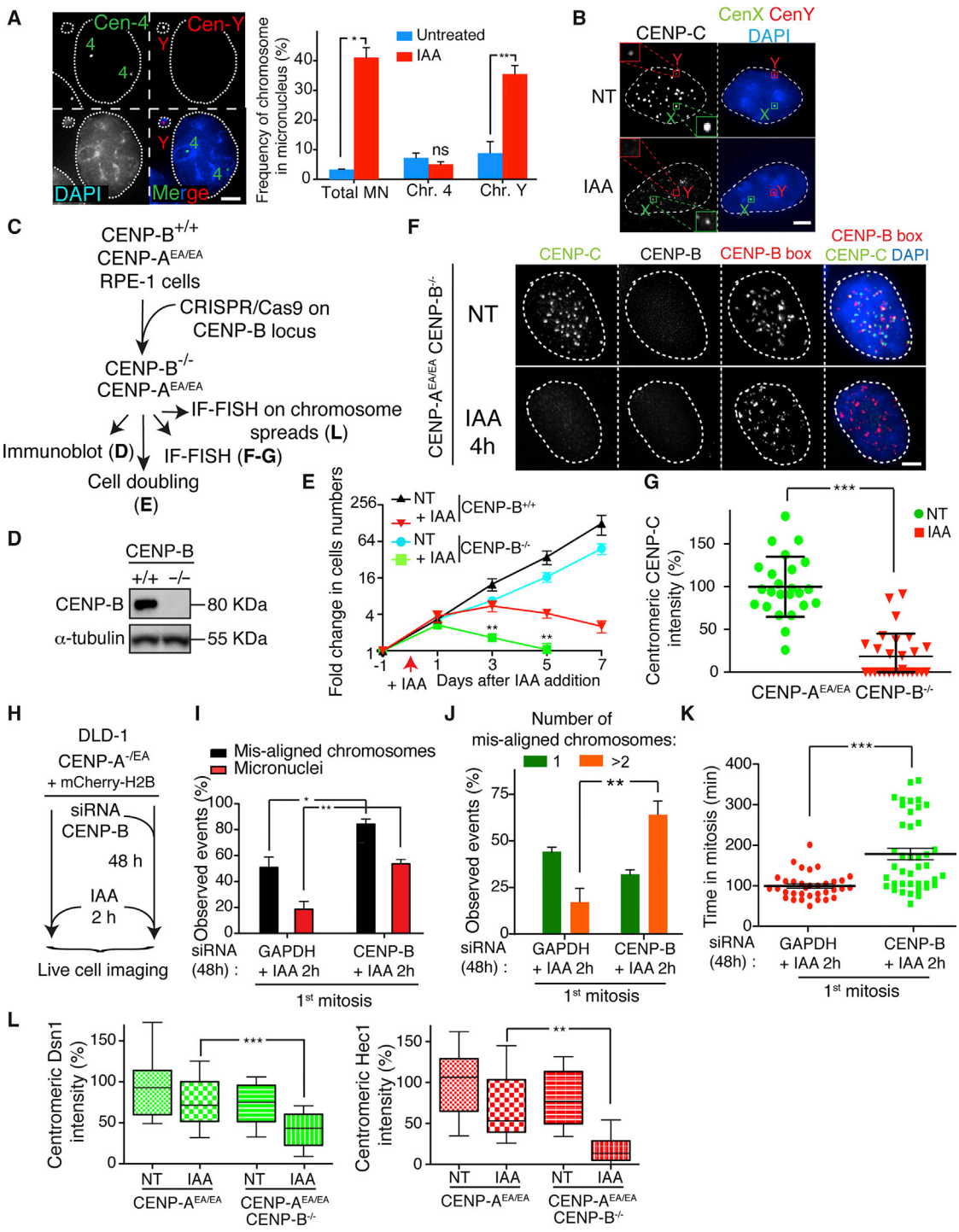

Figure 4. CENP-B Is Sufficient and Essential to Maintain Kinetochore Assembly and Consequently Faithful Chromosome Segregation in the Absence of CENP-A

(A) Representative images show a micronucleus containing the Y chromosome by dual FISH analysis (left). Graphs show the frequency of micronuclei formation (x axis) versus the frequency of a micronucleus containing the chromosome Y or chromosome 4 ± IAA treatment for 24 hr (right). n = ~400 cells. Unpaired t test: *p = 0.01, **p = 0.0094.

(B) Representative images of an immunofluorescence coupled with FISH showed CENP-C binding to centromere on the Y or X chromosome ± IAA treatment for 24 hr. Scale bar, 5 μm.

(C) Schematic of the experimental design shown in (D)–(G).

(legend continued on next page)

centromeric regions. These findings suggest that the majority of single mis-aligned chromosomes in the first mitosis following CENP-A depletion are the Y chromosome.

The preceding results imply that CENP-C-mediated kinetochore assembly stabilized by its binding to CENP-B at centromeric sequences is sufficient to mediate continued kinetochore function and chromosome segregation in the complete absence of CENP-A. To further test this hypothesis, we disrupted both *CENP-B* alleles in the RPE-1 *CENP-A*$^{AE/AE}$ cell line using CRISPR/Cas9-mediated genome editing (Figures 4C and 4D). Without CENP-B, cell lethality was drastically accelerated upon depletion of CENP-A (Figure 4E, compare red triangle with green square lines). Co-depletion of CENP-A and CENP-B abolished centromeric localization of CENP-C and CENP-T (Figures 4F and 4G; Figure S3D). Accordingly, normal CENP-C levels could be restored by expression of an siRNA-resistant, full-length CENP-B rescue construct, but not of a mutant lacking its DNA binding domain (Yoda et al., 1992) and, therefore, its centromeric localization (Figures S3E–S3G). Short-term reduction of CENP-B levels in *CENP-A*$^{-/EA}$ DLD-1 (by siRNA; Figure S3E) caused severe chromosome segregation errors beginning in the first mitosis following CENP-A depletion, with cells accumulating significantly more than one mis-aligned chromosome, developing micronuclei, and displaying an extended mitotic duration (Figures 4H–4K; Movies S2 and S3).

Chromosome segregation failure following CENP-A and CENP-B depletion correlated with rapid dissociation of the kinetochore complex Mis12 (measured by Dsn1 binding) and the Ndc80 complex (measured by Hec1 binding; Figure 4L; Figures S3H and S3I). Altogether, these findings indicate that once the first steps of kinetochore assembly have been completed, centromere and kinetochore components of all chromosomes except the Y are (at least partially) stably maintained in the first mitosis following CENP-A depletion. Furthermore, binding of CENP-B to centromeric DNA is necessary for preserving centromeric CENP-C and faithful chromosome segregation.

Because it has been previously reported that CENP-C is essential for maintaining centromere function (Fukagawa et al., 1999; McKinley et al., 2015) and co-depletion of CENP-A and CENP-B led to CENP-C loss and immediate chromosome mis-segregation (Figure 4), we next tested whether CENP-C was required for retention of mitotic centromere function on pre-assembled kinetochores. To obtain the precise temporal control of inducible CENP-C degradation (missing in previously reported systems; Falk et al., 2015; McKinley et al., 2015), one or both alleles of *CENP-C* were tagged at the C terminus with AID-EYFP in wild-type DLD-1 cells. Addition of IAA rapidly depleted CENP-C (Figures S4A–S4C), suppressed long-term viability (Figure S4D), and induced rapid cell death (Figure S4E). In contrast with CENP-A degradation alone but similar to co-depletion of both CENP-A and CENP-B, depletion of CENP-C resulted in immediate chromosome segregation failure during the first mitosis (Figures S4F–S4H) and rapid de-stabilization of CENP-T and the kinetochore complexes Mis12 and (partially) Ndc80 (Figure S4I). This latter finding extends the previous report of a direct stabilization of CENP-T via CENP-C (Klare et al., 2015). Altogether, these results demonstrate that CENP-C is a key component for direct maintenance of kinetochore architecture and faithful chromosome segregation.

DISCUSSION

We propose a model (Figure 5) in which centromere identity is initially maintained via the CENP-A^{CATD}/HJURP interaction at mitotic exit (Black et al., 2007; Fachinetti et al., 2013; Foltz et al., 2009; Dunleavy et al., 2009). CENP-A deposition is essential to recruit CENP-C in mid-G1 and CENP-N in S-phase (Figures 3A–3F; Figures S2F–S2I; Hellwig et al., 2011). Accordingly, removal of CENP-A in G1 led to an increase in the frequency of chromosome mis-segregation beginning in the next mitosis (Figure 2D). Further, CENP-B binding to α-satellite DNAs in the proximity of CENP-A chromatin enhanced centromeric CENP-C stability (Figure 4; Figure S3G). The CENP-A/CENP-C complex is then required to sustain centromeric CENP-T assembly (which normally occurs in late S-phase; Prendergast et al., 2011) through interdependent interactions among the CCAN subunits (McKinley et al., 2015; Weir et al., 2016). Our data also suggest that CENP-N and CENP-T, both immediately required for cell division (Wood et al., 2016) (Figure S2J), have to cooperate with CENP-C (or at least with its CENP-B-bound fraction) to nucleate a functional kinetochore, in agreement with previous reports (McKinley et al., 2015). Nevertheless, once these centromeric components are assembled, CENP-A is no longer essential for kinetochore tethering to the centromere nor for its function in

(D) Immunoblot shows depletion of endogenous CENP-B using the CRISPR technology. α-Tubulin was used as a loading control.
(E) Cell counting experiment on RPE-1 ± IAA treatment and/or CENP-B gene. IAA was added at day 0 and kept for a maximum of 7 days. Error bars represent the SEM of four independent experiments. Unpaired t test: **p = 0.0043 and 0.0016.
(F) Representative immunofluorescence FISH to measure CENP-C levels following CENP-A depletion (by IAA) in CENP-B-depleted cells. A FISH probe against CENP-B boxes was used to mark centromere position.
(G) Quantification of the experiment shown in (D). Each dot represents an average of 25 centromeres in a single cell. Unpaired t test: ***p < 0.0001.
(H) Schematic of the experiments shown in (I)–(K).
(I) Bar graph shows the percentage of chromosome mis-segregation events observed by live-cell imaging following siRNA depletion of GAPDH or CENP-B and IAA treatment for 2 hr, respectively. Error bars represent the SEM of three independent experiments. Individual n = ~60 cells. Unpaired t test: *p = 0.02, **p = 0.0068.
(J) Bar graph shows the number (1 or >2) of mis-aligned chromosomes in percentage from analysis in (E). Error bars represent the SEM of three independent experiments. Unpaired t test: **p = 0.0093.
(K) Scatterplot graph shows the time in mitosis (from NEBD to chromosome decondensation). Each individual point represents a single cell. Error bars represent the SEM of three independent experiments. Unpaired t test: ***p < 0.0001.
(L) Box and whisker plots of Dsn1 and Hec1 intensities at the centromere measured on metaphase spreads. Unpaired t test: **p = 0.002, ***p = 0.0005.
See also Figures S3 and S4. Scale bars, 5 μm.

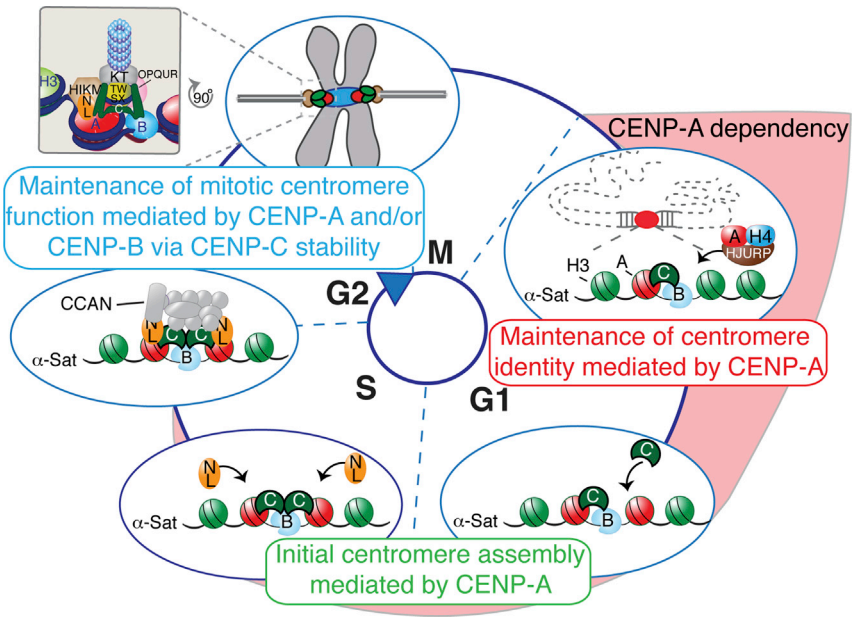

Figure 5. Model of Centromere Function Mediated by Centromeric Chromatin and DNA Sequences

At exit of mitosis, centromeric chromatin replication and identity is mediated by CENP-A (in red) deposition via interaction with HJURP. CENP-A then mediates the assembly of CENP-C (in green) in mid-G1 followed by CENP-N/L (in orange) during S-phase. These steps might be interconnected. At this point, CENP-A becomes dispensable for mitotic centromere function as long as CENP-B (in light blue) is stably bound to centromeric sequences to support CENP-C binding. Assembly of the other subunits of the CCAN, such as CENP-T/W/X/S (in yellow) and HIKM (in light brown), allows the full recruitment of the kinetochore complex (in gray) required to mediate centromere function. In summary, we propose that the kinetochore is tethered to the centromere through a dual linkage of CENP-A chromatin and CENP-B-bound DNA sequences, as the two major links from the DNA to the kinetochore to mediate successful chromosome segregation.

spindle microtubule capture, with the CCAN/kinetochore retained at each centromere (Figure 2; Figure S2C). Thus, although CENP-A depletion after CENP-C/N recruitment alters kinetochore composition in the proximal mitosis, it does not disrupt centromere and kinetochore function in chromosome segregation in that mitosis (Figures 2F and 2G).

These results support an essential role for CENP-A before mitosis in mediating the initial steps of centromere assembly. However, in contrast with CENP-C/-T/-N, CENP-A does not play an active role in centromere-dependent chromosome movement (Figure 5). In support of this model, CENP-C and CENP-T have been reported to be sufficient for kinetochore assembly at ectopic loci (Gascoigne et al., 2011). Furthermore, we now provide evidence that CENP-B binding to α-satellite DNA, previously only proposed to support centromere function (Fachinetti et al., 2015), is indeed sufficient (and essential) for maintenance of a pre-assembled kinetochore and to support chromosome segregation through stabilization of CENP-C (Figure 4).

These findings demonstrate a reciprocal, but non-exclusive, interdependency on centromeric chromatin (marked by CENP-A) and specific centromeric sequences (bound by CENP-B) for tethering the kinetochore complex to centromeres via CENP-C stabilization throughout mitosis. They also involve CENP-B as an important contributor of the CCAN complex to modulate centromere function and strength, which may have implications for karyotypic evolution (Chmátal et al., 2014) due to the variations in the frequency of CENP-B boxes between the centromeres of each mammalian chromosome.

EXPERIMENTAL PROCEDURES

Constructs

osTIR1^{9myc}, H2B^{mRFP}, CENP-N$^{3HA\text{-}SNAP}$, and PCNA^{GFP} were cloned into a pBabe-based vector for retrovirus generation. ^{mCherry}H2B was cloned into a pSMPUW-based vector for lentivirus generation. The FUCCI system was integrated by lentiviral insertion, and clones were selected by FACS. For tetracycline-inducible expression, CENP-T$^{3HA\text{-}SNAP}$, siRNA-resistant CENP-B-GFP or $^{\Delta NH2}$CENP-B-GFP was cloned into a pcDNA5/FRT/TO-based vector (Invitrogen).

Cell Culture Conditions

Cells were maintained at 37°C in a 5% CO_2 atmosphere. Flp-In TRex-DLD-1 were grown in DMEM containing 10% tetracycline-free fetal bovine serum (GE Healthcare), 100 U/ml penicillin, 100 U/ml streptomycin, and 2 mM L-glutamine, whereas hTERT RPE-1 cells were maintained in DMEM:F12 medium containing 10% tetracycline-free fetal bovine serum (Pan Biotech), 0.348% sodium bicarbonate, 100 U/ml penicillin, 100 U/ml streptomycin, and 2 mM L-glutamine. IAA (I5148; Sigma) was used at 500 μM, Colcemid (Roche) and nocodazole (Sigma) were used at 0.1 mg/ml, thymidine at 2 mM, doxycycline (Sigma) at 1 mg/ml, and palbociclib at 1 μM. Cold treatment experiment to determine kinetochore and microtubules stability was performed for 15 min on ice.

Generation of Stable Cell Lines

Stable, isogenic cell lines expressing CENP-B-GFP FL or ΔN were generated using the FRT/Flp-mediated recombination system as described previously (Fachinetti et al., 2013). The different transgenes used in this study were introduced by retroviral delivery as described previously (Fachinetti et al., 2013). Stable integration was selected with 5 μg/ml puromycin or 10 μg/ml blasticidin S, and single clones were isolated using fluorescence-activated cell sorting (FACS Vantage; Becton Dickinson).

siRNA, SNAP-Tagging, Clonogenic Colony Assay, and Cell Counting Experiments

siRNAs were introduced using Lipofectamine RNAiMax (Invitrogen). A pool of four siRNAs directed against CENP-B and GAPDH (Fachinetti et al., 2013) was purchased from Dharmacon. SNAP labeling was conducted as described previously (Jansen et al., 2007). Clonogenic colony assays were done as described previously (Fachinetti et al., 2013). For the counting experiment, cells were plated at 1 × 10^5 cells/mL in a six-well plate. After 24 hr, auxin was added to the medium. Cells were then counted and divided every other day for 7 days.

Gene Targeting

Transcription activator-like effector nucleases (TALENs) were assembled using the Golden Gate cloning strategy and library as described previously

(Fachinetti et al., 2015) and cloned into a modified version of pcDNA3.1 (Invitrogen) containing also the Fok I endonuclease domain as previously described (Fachinetti et al., 2015). TALENs were designed to the N-terminal region of CENP-A gene: 5′-GTCATGGGCCCGCGCC-3′ and 5′-GGCCCC GAGGAGGCGCA-3′. RPE-1 and DLD-1 cells were co-transfected with the TALEN expression vectors and the donor cassette (containing the two homology arms for CENP-A N-terminal region and the AID and EYFP gene) by nucleofection (Lonza), and positive clones were selected by FACS. CENP-C targeting was done as previously described (Fachinetti et al., 2015). CENP-B gene was deleted as described before (Fachinetti et al., 2015).

Surveyor Nuclease Assay

A surveyor nuclease assay was performed as previously described (Fachinetti et al., 2015). In brief, 1×10^6 U2OS cells were transfected with 1,000 ng of the small guide RNA (sgRNA)/Cas9 expression vector by nucleofection (Lonza) using program X-001 and a nucleofection buffer (100 mM KH_2PO_4, 15 mM $NaHCO_3$, 12 mM $MgCl_2$, 6 H_2O, 8 mM ATP, 2 mM glucose [pH 7.4]). Forty-eight hours following transfection, genomic DNA was isolated using the quick g-DNA miniprep isolation kit (Zymo), and PCR was performed using Q5 polymerase (NEB) with CENP-A-specific primers sitting just outside of the target sequence (forward primer: 5′-GACTTCTGCCAAGCACCG-3′; reverse primer: 5′-GCCTCGGTTTTCTCCTCTTC-3′). PCR products were denatured, annealed, treated with the surveyor nuclease (Transgenomic), separated on a 10% Tris-borate-EDTA (TBE) polyacrylamide gel, and visualized by ethidium bromide staining.

Immunoblotting

For immunoblot analysis, protein samples were separated by SDS-PAGE, transferred onto nitrocellulose membranes (Bio-Rad), and then probed with the following antibodies: DM1A (α-tubulin, 1:5,000), CENP-A (1:1,000; Cell Signaling), GFP (1:1,000; Cell Signaling), HJURP (1:1,000; Covance) (Foltz et al., 2009), CENP-B (1:1,000; Abcam and Upstate), GAPDH (1:10,000; Abcam), CENP-C (a gift from Iain Cheeseman, MIT, Boston, and Ben Black, University of Pennsylvania, Philadelphia), c-Myc (1:1,000; Sigma), and H4 (1:250; Abcam).

Immunofluorescence, Chromosome Spreads, Live-Cell Microscopy, and IF-FISH

Cells were fixed in 4% formaldehyde at room temperature or in methanol at −20°C for 10 min. Incubations with primary antibodies were conducted in blocking buffer for 1 hr at room temperature using the following antibodies: CENP-A (1:1,500; Abcam), CENP-C (1:1,000; MBL), CENP-B (1:1,000; Abcam), ACA (1:500; Antibodies), Hec1 (1:1,000; Abcam), Dsn1 (1:1000, a gift from A. Desai, Ludwig Institute for Cancer Research, San Diego), CENP-I (a gift from Song-Tao Liu, University of Toledo), DM1A (α-tubulin, 1:2,000), CENP-T (1:5,000; Covance), and HA-11 (1:1,000; Covance). Immunofluorescence on chromosome spreads was done as described previously (Fachinetti et al., 2015). Immunofluorescence images were collected using a Deltavision Core system (Applied Precision). For live-cell imaging, cells were plated on high optical quality plastic slides (ibidi) and imaged using a Deltavision Core system (Applied Precision) or spinning disk with deconvolution and denoising (Nikon). For IF-FISH, we follow the IF protocol followed by the FISH protocol (see later).

FISH Experiment

Cells were fixed in Carnoy's fixative (methanol/acetic acid 3:1) for 15 min at room temperature, rinsed in 80% ethanol, and air-dried for 5 min. Probe mixtures (MetaSystems) were applied and sealed with a coverslip. Slides were denatured at 75°C for 2 min and incubated at 37°C overnight in a humidified chamber. Slides were washed with 0.4X saline sodium citrate buffer (SSC) at 72°C for 2 min, 4X SSC, 0.1% Tween 20 at room temperature for 30 s, and rinsed with PBS. Slides were incubated with DAPI solution for 10 min before mounting in anti-fade reagent.

Centromere Quantification

Centromere quantifications on interphase cells: quantification of centromere signal intensity on interphase cells was done manually as described previously (Fachinetti et al., 2013) or using an automated system (Fachinetti et al., 2015). In brief, for the manual quantification, un-deconvolved 2D maximum intensity projections were saved as un-scaled 16-bit TIFF images, and signal intensities were determined using MetaMorph (Molecular Devices). A 15 × 15 pixel circle was drawn around a centromere (marked by ACA or CENP-B staining), and an identical circle was drawn adjacent to the structure (background). The integrated signal intensity of each individual centromere was calculated by subtracting the fluorescence intensity of the background from the intensity of the adjacent centromere. Twenty-five centromeres were averaged to provide the average fluorescence intensity for each individual cell, and more than 30 cells were quantified per experiment.

Chromatin Extraction and Affinity Purification

Nuclei from 1×10^9 DLD-1 cells were prepared as previously described (Foltz et al., 2006), except for reducing the NaCl to 150 mM in the wash buffer. Chromatin was digested at room temperature using 140 U/mL micrococcal nuclease (catalog no. 10107921001; Roche) for 20 min to produce mono-nucleosomes and short oligo-nucleosomes of up to three nucleosomes or for 35 min to produce a pool of mono-nucleosomes. Following micrococcal nuclease treatment, extracts were supplemented with 5 mM EGTA and 0.05% Nonidet P-40 (NP-40) and centrifuged at 10,000 × *g* for 15 min at 4°C.

For affinity purification, GFP-tagged chromatin was immunoprecipitated using mouse anti-GFP antibody (clones 19C8 and 19F7; Monoclonal Antibody Core Facility at Memorial Sloan Kettering Cancer Center) coupled to Dynabeads M-270 Epoxy (catalog no. 14301; Life Technologies). Chromatin extracts were incubated with antibody-bound beads for 16 hr at 4°C. Bound complexes were washed once in buffer A (20 mM HEPES [pH 7.7], 20 mM KCl, 0.4 mM EDTA, and 0.4 mM DTT), once in buffer A with 300 mM KCl, and finally twice in buffer A with 300 mM KCl, 1 mM DTT, and 0.1% Tween 20.

DNA Extraction

Following elution of the chromatin from the beads, proteinase K (100 μg/ml) was added and samples were incubated for 2 hr at 55°C. DNA was purified from proteinase K-treated samples using a DNA purification kit following the manufacturer's instructions (Promega) and was subsequently analyzed by running a 2% low-melting agarose (APEX) gel.

Chromatin Immunoprecipitation and qPCR Analysis

Cells were crosslinked in 0.75% formaldehyde for 10 min at room temperature. The reaction was stopped by adding 125 mM glycine for 5 min at room temperature. Chromatin was fragmented by sonication in a ChIP buffer (50 mM 4-(2-hydroxyethyl)-1-piperazineethanesulfonic acid - potassium hydroxide [HEPES-KOH; pH 7.5], 140 mM NaCl, 1 mM EDTA [pH 8], 1% Triton X-100, 0.1% sodium deoxycholate, 0.1% SDS). The soluble chromatin was diluted 1:10 with RIPA buffer (50 mM Tris HCl [pH 7.6], 150 mM NaCl, 1 mM EDTA, 1% NP-40, 1% sodium deoxycholate, 0.1% SDS, 1% protease inhibitor), pre-cleared with Dynabeads Protein G (Thermo Fisher Scientific) and immunoprecipitated overnight at 4°C with anti-CENP-C (MBL). Chromatin was then washed once in low-salt wash buffer (0.1% SDS, 1% Triton X-100, 2 mM EDTA, 50 mM Tris HCl [pH 7.6]), once in high-salt wash buffer (0.1% SDS, 1% Triton X-100, 2 mM EDTA, 20 mM Tris HCl [pH 7.6], 500a mM NaCl), and once in LiCl wash buffer (0.25 M LiCl, 1% NP-40, 1% sodium deoxycholate, 1 mM EDTA, 10 mM Tris HCl). Samples were eluted with elution buffer at 30°C for 15 min and then incubated at 65°C overnight with 5 M NaCl. Then samples were incubated with 10 mg/ml RNase A and 20 mg/ml Proteinase K for 1 hr at 45°C and DNA was purified by phenol-chloroform. The recovered DNA and the soluble chromatin (input) were quantified by qPCR using the LightCycler 480 (Roche). The following primers were used to amplify Y centromere (Fw: 5′-TCCTTTTCCACAATAGACGTCA-3′; Rev: 5′-GGAAGTATCTT CCCTTAAAAGCTATG-3′), Telomere (Fw: 5′-ACACTAAGGTTTGGGTTTGGG TTTGGGTTTGGGTTAGTGT-3′; Rev: 5′-TGTTAGGTATCCCTATCCCTATCCC TATCCCTATCCCTAACA-3′), satellite 2 (Fw: 5′-CTGCACTACCTGAAGAG GAC-3′; Rev: 5′-GATGGTTCAACACTCTTACA-3′), 17 centromere (Fw: 5′-CAACTCCCAGAGTTTCACATTGC-3′; Rev: 5′-GGAAACTGCTCTTTGAAAAG GAACC-3′), and alpha satellite (Fw: 5′-TCATTCCCACAAACTGCGTTG-3′; Rev: 5′-TCCAACGAAGGCCACAAGA-3′).

Statistical Methods

Statistical analysis of all the graphs was performed using the unpaired t test in Prism 6 in which the following parameters were considered: p value, p value summary, significant difference ($p < 0.05$), two-tailed p value and "t, df" values.

SUPPLEMENTAL INFORMATION

Supplemental Information includes four figures and three movies and can be found with this article online at http://dx.doi.org/10.1016/j.celrep.2016.10.084.

AUTHOR CONTRIBUTIONS

D.F. conceived the experimental design. D.F. and M.A.M. performed gene-targeting of CENP-A and CENP-C. Y.N.-A. performed affinity purification experiments. P.L. performed the micronuclei experiment on the Y chromosome and contributed to text editing. V.B. performed CENP-A depletion on synchronized cells. V.B. and S.H. carried out ChIP analysis of CENP-C. S.H., M.D., and D.F. performed and analyzed all the remaining experiments. D.F. and D.W.C. wrote the manuscript and secured funding.

ACKNOWLEDGMENTS

The authors would like to thank B.E. Black (University of Pennsylvania, Philadelphia), C. Bartocci (Institut Curie, Paris), Dong Hyun Kim (Ludwig Institute for Cancer Research, La Jolla), Amira Abdullah (Ludwig Institute for Cancer Research), and Vincent Fraisier (Institut Curie) for helpful suggestions and technical help, and K. McKinley and I. Cheeseman (MIT, Boston), A. Desai (Ludwig Institute for Cancer Research), G. Orsi and G. Almouzni (Institut Curie), I. Draskovic and A. Londono (Institut Curie), Song-Tao Liu (University of Toledo), A. Miyawaki (Hirosawa), and B.E. Black (University of Pennsylvania) for providing reagents. We also thank the FACS facility in the Sanford Consortium for Regenerative Medicine (La Jolla) and the PICT imaging platform at Institut Curie, part of the national infrastructure France-BioImaging (grant ANR-10-INSB-04). D.W.C. has received support from NIH grant R01 GM074150. D.W.C. receives salary support from the Ludwig Institute for Cancer Research. D.F. receives salary support from the CNRS. D.F. has received support by Labex "CelTisPhyBio," the Institut Curie, and the ATIP-Avenir 2015 program. This work has also received support under the program "Investissements d'Avenir," launched by the French Government and implemented by ANR with the references ANR-10-LABX-0038 and ANR-10-IDEX-0001-02 PSL.

Received: May 5, 2016
Revised: September 22, 2016
Accepted: October 25, 2016
Published: November 22, 2016

REFERENCES

Bade, D., Pauleau, A.L., Wendler, A., and Erhardt, S. (2014). The E3 ligase CUL3/RDX controls centromere maintenance by ubiquitylating and stabilizing CENP-A in a CAL1-dependent manner. Dev. Cell *28*, 508–519.

Black, B.E., Foltz, D.R., Chakravarthy, S., Luger, K., Woods, V.L., Jr., and Cleveland, D.W. (2004). Structural determinants for generating centromeric chromatin. Nature *430*, 578–582.

Black, B.E., Jansen, L.E., Maddox, P.S., Foltz, D.R., Desai, A.B., Shah, J.V., and Cleveland, D.W. (2007). Centromere identity maintained by nucleosomes assembled with histone H3 containing the CENP-A targeting domain. Mol. Cell *25*, 309–322.

Bodor, D.L., Rodríguez, M.G., Moreno, N., and Jansen, L.E. (2012). Analysis of protein turnover by quantitative SNAP-based pulse-chase imaging. Curr. Protoc. Cell Biol. *Chapter 8*, Unit8.8.

Bodor, D.L., Mata, J.F., Sergeev, M., David, A.F., Salimian, K.J., Panchenko, T., Cleveland, D.W., Black, B.E., Shah, J.V., and Jansen, L.E. (2014). The quantitative architecture of centromeric chromatin. eLife *3*, e02137.

Carroll, C.W., Silva, M.C., Godek, K.M., Jansen, L.E., and Straight, A.F. (2009). Centromere assembly requires the direct recognition of CENP-A nucleosomes by CENP-N. Nat. Cell Biol. *11*, 896–902.

Carroll, C.W., Milks, K.J., and Straight, A.F. (2010). Dual recognition of CENP-A nucleosomes is required for centromere assembly. J. Cell Biol. *189*, 1143–1155.

Cheeseman, I.M., and Desai, A. (2008). Molecular architecture of the kinetochore-microtubule interface. Nat. Rev. Mol. Cell Biol. *9*, 33–46.

Chmátal, L., Gabriel, S.I., Mitsainas, G.P., Martínez-Vargas, J., Ventura, J., Searle, J.B., Schultz, R.M., and Lampson, M.A. (2014). Centromere strength provides the cell biological basis for meiotic drive and karyotype evolution in mice. Curr. Biol. *24*, 2295–2300.

Dunleavy, E.M., Roche, D., Tagami, H., Lacoste, N., Ray-Gallet, D., Nakamura, Y., Daigo, Y., Nakatani, Y., and Almouzni-Pettinotti, G. (2009). HJURP is a cell-cycle-dependent maintenance and deposition factor of CENP-A at centromeres. Cell *137*, 485–497.

Earnshaw, W.C., Ratrie, H., 3rd, and Stetten, G. (1989). Visualization of centromere proteins CENP-B and CENP-C on a stable dicentric chromosome in cytological spreads. Chromosoma *98*, 1–12.

Fachinetti, D., Folco, H.D., Nechemia-Arbely, Y., Valente, L.P., Nguyen, K., Wong, A.J., Zhu, Q., Holland, A.J., Desai, A., Jansen, L.E., and Cleveland, D.W. (2013). A two-step mechanism for epigenetic specification of centromere identity and function. Nat. Cell Biol. *15*, 1056–1066.

Fachinetti, D., Han, J.S., McMahon, M.A., Ly, P., Abdullah, A., Wong, A.J., and Cleveland, D.W. (2015). DNA sequence-specific binding of CENP-B enhances the fidelity of human centromere function. Dev. Cell *33*, 314–327.

Falk, S.J., Guo, L.Y., Sekulic, N., Smoak, E.M., Mani, T., Logsdon, G.A., Gupta, K., Jansen, L.E., Van Duyne, G.D., Vinogradov, S.A., et al. (2015). Chromosomes. CENP-C reshapes and stabilizes CENP-A nucleosomes at the centromere. Science *348*, 699–703.

Foltz, D.R., Jansen, L.E., Black, B.E., Bailey, A.O., Yates, J.R., 3rd, and Cleveland, D.W. (2006). The human CENP-A centromeric nucleosome-associated complex. Nat. Cell Biol. *8*, 458–469.

Foltz, D.R., Jansen, L.E., Bailey, A.O., Yates, J.R., 3rd, Bassett, E.A., Wood, S., Black, B.E., and Cleveland, D.W. (2009). Centromere-specific assembly of CENP-a nucleosomes is mediated by HJURP. Cell *137*, 472–484.

Fukagawa, T., and Earnshaw, W.C. (2014). The centromere: chromatin foundation for the kinetochore machinery. Dev. Cell *30*, 496–508.

Fukagawa, T., Pendon, C., Morris, J., and Brown, W. (1999). CENP-C is necessary but not sufficient to induce formation of a functional centromere. EMBO J. *18*, 4196–4209.

Gascoigne, K.E., Takeuchi, K., Suzuki, A., Hori, T., Fukagawa, T., and Cheeseman, I.M. (2011). Induced ectopic kinetochore assembly bypasses the requirement for CENP-A nucleosomes. Cell *145*, 410–422.

Guse, A., Carroll, C.W., Moree, B., Fuller, C.J., and Straight, A.F. (2011). In vitro centromere and kinetochore assembly on defined chromatin templates. Nature *477*, 354–358.

Hellwig, D., Emmerth, S., Ulbricht, T., Döring, V., Hoischen, C., Martin, R., et al. (2011). Dynamics of CENP-N kinetochore binding during the cell cycle. J. Cell. Sci. *124* (*Pt 22*), 3871–3883.

Holland, A.J., Fachinetti, D., Han, J.S., and Cleveland, D.W. (2012). Inducible, reversible system for the rapid and complete degradation of proteins in mammalian cells. Proc. Natl. Acad. Sci. USA *109*, E3350–E3357.

Hori, T., Amano, M., Suzuki, A., Backer, C.B., Welburn, J.P., Dong, Y., McEwen, B.F., Shang, W.H., Suzuki, E., Okawa, K., et al. (2008). CCAN makes multiple contacts with centromeric DNA to provide distinct pathways to the outer kinetochore. Cell *135*, 1039–1052.

Izuta, H., Ikeno, M., Suzuki, N., Tomonaga, T., Nozaki, N., Obuse, C., Kisu, Y., Goshima, N., Nomura, F., Nomura, N., and Yoda, K. (2006). Comprehensive analysis of the ICEN (Interphase Centromere Complex) components enriched in the CENP-A chromatin of human cells. Genes Cells *11*, 673–684.

Jansen, L.E.T., Black, B.E., Foltz, D.R., and Cleveland, D.W. (2007). Propagation of centromeric chromatin requires exit from mitosis. J. Cell Biol. *176*, 795–805.

Kato, H., Jiang, J., Zhou, B.R., Rozendaal, M., Feng, H., Ghirlando, R., Xiao, T.S., Straight, A.F., and Bai, Y. (2013). A conserved mechanism for centromeric nucleosome recognition by centromere protein CENP-C. Science *340*, 1110–1113.

Klare, K., Weir, J.R., Basilico, F., Zimniak, T., Massimiliano, L., Ludwigs, N., Herzog, F., and Musacchio, A. (2015). CENP-C is a blueprint for constitutive centromere-associated network assembly within human kinetochores. J. Cell Biol. *210*, 11–22.

Liu, S.T., Rattner, J.B., Jablonski, S.A., and Yen, T.J. (2006). Mapping the assembly pathways that specify formation of the trilaminar kinetochore plates in human cells. J. Cell Biol. *175*, 41–53.

Logsdon, G.A., Barrey, E.J., Bassett, E.A., DeNizio, J.E., Guo, L.Y., Panchenko, T., Dawicki-McKenna, J.M., Heun, P., and Black, B.E. (2015). Both tails and the centromere targeting domain of CENP-A are required for centromere establishment. J. Cell Biol. *208*, 521–531.

McKinley, K.L., and Cheeseman, I.M. (2016). The molecular basis for centromere identity and function. Nat. Rev. Mol. Cell Biol. *17*, 16–29.

McKinley, K.L., Sekulic, N., Guo, L.Y., Tsinman, T., Black, B.E., and Cheeseman, I.M. (2015). The CENP-L-N complex forms a critical node in an integrated meshwork of interactions at the centromere-kinetochore interface. Mol. Cell *60*, 886–898.

Miga, K.H., Newton, Y., Jain, M., Altemose, N., Willard, H.F., and Kent, W.J. (2014). Centromere reference models for human chromosomes X and Y satellite arrays. Genome Res. *24*, 697–707.

Nishimura, K., Fukagawa, T., Takisawa, H., Kakimoto, T., and Kanemaki, M. (2009). An auxin-based degron system for the rapid depletion of proteins in nonplant cells. Nat. Methods *6*, 917–922.

Okada, M., Cheeseman, I.M., Hori, T., Okawa, K., McLeod, I.X., Yates, J.R., 3rd, Desai, A., and Fukagawa, T. (2006). The CENP-H-I complex is required for the efficient incorporation of newly synthesized CENP-A into centromeres. Nat. Cell Biol. *8*, 446–457.

Prendergast, L., van Vuuren, C., Kaczmarczyk, A., Doering, V., Hellwig, D., Quinn, N., Hoischen, C., Diekmann, S., and Sullivan, K.F. (2011). Premitotic assembly of human CENPs -T and -W switches centromeric chromatin to a mitotic state. PLoS Biol. *9*, e1001082.

Régnier, V., Vagnarelli, P., Fukagawa, T., Zerjal, T., Burns, E., Trouche, D., Earnshaw, W., and Brown, W. (2005). CENP-A is required for accurate chromosome segregation and sustained kinetochore association of BubR1. Mol. Cell. Biol. *25*, 3967–3981.

Sakaue-Sawano, A., Kurokawa, H., Morimura, T., Hanyu, A., Hama, H., Osawa, H., Kashiwagi, S., Fukami, K., Miyata, T., Miyoshi, H., et al. (2008). Visualizing spatiotemporal dynamics of multicellular cell-cycle progression. Cell *132*, 487–498.

Shelby, R.D., Vafa, O., and Sullivan, K.F. (1997). Assembly of CENP-A into centromeric chromatin requires a cooperative array of nucleosomal DNA contact sites. J. Cell Biol. *136*, 501–513.

Smoak, E.M., Stein, P., Schultz, R.M., Lampson, M.A., and Black, B.E. (2016). Long-term retention of CENP-A nucleosomes in mammalian oocytes underpins transgenerational inheritance of centromere identity. Curr. Biol. *26*, 1110–1116.

Tachiwana, H., Müller, S., Blümer, J., Klare, K., Musacchio, A., and Almouzni, G. (2015). HJURP involvement in de novo CenH3(CENP-A) and CENP-C recruitment. Cell Rep. *11*, 22–32.

Weir, J.R., Faesen, A.C., Klare, K., Petrovic, A., Basilico, F., Fischböck, J., Pentakota, S., Keller, J., Pesenti, M.E., Pan, D., et al. (2016). Insights from biochemical reconstitution into the architecture of human kinetochores. Nature *537*, 249–253.

Wood, L., Booth, D.G., Vargiu, G., Ohta, S., deLima Alves, F., Samejima, K., Fukagawa, T., Rappsilber, J., and Earnshaw, W.C. (2016). Auxin/AID versus conventional knockouts: distinguishing the roles of CENP-T/W in mitotic kinetochore assembly and stability. Open Biol. *6*, 150230.

Yoda, K., Kitagawa, K., Masumoto, H., Muro, Y., and Okazaki, T. (1992). A human centromere protein, CENP-B, has a DNA binding domain containing four potential alpha helices at the NH2 terminus, which is separable from dimerizing activity. J. Cell Biol. *119*, 1413–1427.